^{15}N Chemical Shift Principal Values in Nitrogen Heterocycles

Mark S. Solum,[†] Karen L. Altmann,[‡] Mark Strohmeier,[‡] David A. Berges,[§] Yulei Zhang,[§] Julio C. Facelli,[‡,⊥] Ronald J. Pugmire,*[,†] and David M. Grant*[,‡]

Contribution from the Departments of Chemical and Fuels Engineering and Chemistry, and Center for High Performance Computing, University of Utah, Salt Lake City, Utah 84112, and Department of Chemistry and Biochemistry, Brigham Young University, Provo, Utah 84602

Received December 2, 1996. Revised Manuscript Received May 6, 1997[⊗]

Abstract: This paper presents data on the ^{15}N chemical shift tensor principal values in a series of ^{15}N-enriched heterocycles. Compounds that are liquids at room temperature were frozen, and the principal values of all compounds studied were measured from static powder patterns. Four different types of nitrogen tensors are described, consisting of protonated and nonprotonated nitrogens in both five- and six-membered rings. The principal values were oriented on the molecular frame using the DFT quantum mechanical calculations of the ^{15}N chemical shielding tensors. The agreement between the calculated and experimental principal values is adequate to make these assignments, but the relative scatters are greater than those observed in similar ^{13}C chemical shift calculations. The largest shift component, δ_{11}, is always oriented in the radial direction to the ring for substituted nitrogens but is tangential to the ring for the nonsubstituted nitrogens. The large variations observed in the nitrogen chemical shift tensors upon changing the nitrogen hybridization can be explained using qualitative arguments on the localization of the smallest bonding-antibonding or HOMO−LUMO gap in the molecule. The orientation of the largest shift component is always found in the plane of the molecule and is approximately perpendicular to the plane containing the bonding−antibonding or HOMO−LUMO pair of orbitals with the smallest energy gap.

Introduction

During the past 15 years solid state NMR spectroscopy and its applications have grown rapidly in chemical popularity. The availability of new commercial instrumentation and experimental techniques, designed specifically for the study of solids, has opened up new areas that have previously been unavailable to the broader chemical community. While the majority of such applications have utilized ^{13}C nuclei for the study of solid materials, a much broader range of interesting nuclei (e.g., ^{11}B, ^{14}N, ^{15}N, ^{17}O, ^{19}F, ^{23}Na, ^{27}Al, ^{29}Si, ^{31}P, ^{113}Cd, ^{209}Pb, etc.) is now emerging for use by solid state scientists. While the isotropic chemical shifts of nuclear spins provide valuable chemical information, the principal values of the shift tensor in the solid state reveal even more information regarding the subtle differences in electronic and geometrical structural characteristics.[1] To date, the great majority of chemical shift tensor data appearing in the literature has been on the ^{13}C nucleus.[2]

Nitrogen NMR data have been extensively reviewed by Witanowski et al.[3] and by Mason.[4] Most of the literature describes isotropic shifts and their relationship to structure elucidation, the importance of solvent effects, and tautomeric equilibria. The combination of a large shift range, approximately 1100 ppm in organic compounds,[3] and sensitivity to electronic interactions involving the lone pair make ^{15}N shifts a very sensitive probe of both structural changes and intermolecular interactions.[5] A significant amount of attention has recently been focused on the role of nitrogen in biological structures[6] because of its sensitivity to both hydrogen bonding and intermolecular and long range interactions. This paper begins to lay the foundation for using ^{15}N shift tensor information to elucidate the structure of nitrogen-containing substances in such diverse solids as nucleic acids and fossil fuels. The ^{15}N chemical shift principal values in these types of nitrogen heterocycles are present with great diversity in these materials.[7]

The extent of ^{15}N NMR studies in solids have been limited due to the low sensitivity and long spin−lattice relaxation times of ^{15}N nuclei. Consequently, there is very little information on the chemical shift principal values of nitrogens in different environments. Most of the reports in the literature are on chemical shift tensors for sp^3 nitrogens with modest anisotropies.[2−4] A number of ^{15}N chemical shift tensors or their principal values have been reported for substituted pyrazines,[8] uracil,[9] benzimidazole and cytosine,[10] *cis*-azobenzene,[11] nitroso groups,[12] nitrate and nitrite ions,[13] and benzamide.[5]

This paper is the first extensive report of the principal values of ^{15}N chemical shift tensors in a series of related five- and six-membered nitrogen heterocycles. Several ionic species have been included in this study to evaluate the effects of nitrogen protonation as well as ring size (five- vs six-membered). It is noted that four different types of nitrogen tensors are found in

[†] Department of Chemical and Fuels Engineering, University of Utah.
[‡] Department of Chemistry, University of Utah.
[§] Brigham Young University.
[⊥] Center for High Performance Computing, University of Utah.
[⊗] Abstract published in *Advance ACS Abstracts,* August 1, 1997.

(1) Facelli, J. C. Shielding Tensor Calculations. In *Encyclopedia of Nuclear Magnetic Resonance*; Grant, D. M., Harris, R. K., Eds.; John Wiley: London, 1996; p 4327.
(2) Duncan, T. M. *A Compilation of Chemical Shift Anisotropies*. The Farragut Press: Chicago, 1990.
(3) Witanowski, M.; Stefaniak, L.; Webb, G. A. Nitrogen NMR Spectroscopy. In *Annual Reports on NMR Spectroscopy*; Webb, G. A., Ed.; Academic Press: London, 1993; Vol. 25, p 2 and previous reviews of these authors in this series.
(4) Mason, J. Nitrogen NMR. In *Encyclopedia of Nuclear Magnetic Resonance*; Grant, D. M., Harris, R. K., Eds.; John Wiley: London, 1996; p 3222.
(5) Facelli, J. C.; Pugmire, R. J.; Grant, D. M. *J. Am. Chem. Soc.* **1996**, *118*, 5488.
(6) See, for example: (a) Teng, Q.; Iqbal, M.; Cross, T. A. *J. Am. Chem. Soc.* **1992**, *114*, 5312. (b) Shoji, A.; Ozaki, T.; Fujito, T.; Deguchi, K.; Ando, I. Ando, S. *J. Am. Chem. Soc.* **1990**, *112*, 4693. (c) Le, H.; Oldfield, E. *J. Biomol. NMR* **1994**, *4*, 341.
(7) Smith, K. L.; Smoot, L. D.; Fletcher, T. H.; Pugmire, R. J. *The Structure and Reaction Processes of Coal*; Plenum: New York, 1994. Morrison, R. T.; Boyd, R. N. *Organic Chemistry*, 4th ed.; Allyn and Bacon: Boston, 1983; Chapters 31 and 35.
(8) Hoelger, C. G.; Aguilar-Parrilla; F. Elguero, J.; Weintraub, O.; Vega, S.; Limbach, H. H. *J. Magn. Reson.* **1996**, *A120*, 46.

S0002-7863(96)04135-2 CCC: $14.00

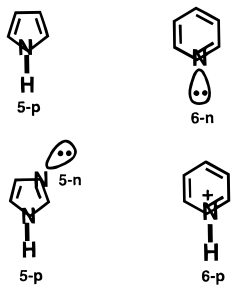

Figure 1. Definition of the different types of nitrogen atoms present in five- and six-membered nitrogen heterocycles. The terms "n" and "p" represent nonbonded lone pair and protonated, or bonded, lone pair.

simple heterocyclic systems. For convenience, the nitrogens with nonbonded lone electron pairs in six- and five-membered heterocyclic rings shall be referred to as **6-n** and **5-n** types of nitrogens, respectively. The **5-p** designation is used to designate those nitrogens which are substituted (e.g., with hydrogen or alkyl groups) such as observed in pyrrole and imidazole type heterocycles, and **6-p** designates substituted nitrogens in six-membered heterocycles (see Figure 1). Quantum mechanical calculations were used to assign the principal values to the molecular frame and to provide insight into the effects of electronic structure on the chemical shielding.

Experimental Section

Sample Preparation. ^{15}N labeled (at the 98% level) compounds were obtained from commercial sources: pyridine-^{15}N (Isotec, Inc.), pyrrole-^{15}N (Cambridge Isotope Laboratories), and imidazole-^{15}N (Icon Services, Inc.) were prepared following standard procedures as described below.

1-Methylpyridinium-^{15}N Methanesulfonate. A mixture of pyridine-^{15}N (1.0 mL) and 3.54 mL of methyl methanesulfonate in 10 mL of benzene (dried over CaH_2) was slowly heated to boiling and refluxed for 30 min. After having been cooled the product was collected by filtration and recrystallized from ethanol/ethyl acetate. Yield: 2.2 g (93%). Mp 131−132 °C. Anal. Calcd for $C_7H_{11}{}^{15}NO_3S$: C, 44.20; H, 5.83; N, 7.89. Found: C, 44.42; H, 6.02; N, 7.70. ^1H NMR (D_2O) δ: 9.27 (d, 2H), 8.43 (t, 1H), 8.06 (t, 2H), 4.6 (s, 3H), 2.75 (s, 1H).

Pyridine-^{15}N-1-oxide. The compound was synthesized from 1.0 mL of pyridine-^{15}N according to a literature procedure[14] for the unlabeled compound and crystallized upon drying under vacuum for 2 days. Yield: 0.82 g (70%). Mp 64−66 °C (lit. 65 °C). ^1H NMR ($CDCl_3$) δ: 8.31 (d, 2H), 7.35 (t, 3H).

Imidazole-^{15}N Hydrochloride. To a solution of imidazole-^{15}N (0.2 g, 2.94 mmol) in 20 mL of anhydrous THF was added a solution of 1.15 mL (2.94 mmol) of 2.55 M hydrogen chloride in anhydrous diethyl ether slowly with stirring. After 20 min at room temperature a white solid was collected by filtration and washed under nitrogen with anhydrous THF (3 × 4 mL) and then anhydrous hexane (3 × 4 mL). The compound was dried and stored over P_2O_5. Yield: 0.28 g (91%). Mp 158 °C, lit. value[15] 160−163°C. ^1H NMR (D_2O) δ: 8.67 (s, 1H), 7.46 (s, 2H).

Lithium Pyrrolate-^{15}N. To a stirred solution of 0.2 mL of pyrrole-^{15}N (2.9 mmol) in 10 mL of anhydrous hexane was slowly added 1.2 mL of 2.5 M butyllithium (3 mmol) in hexane at room temperature and under nitrogen. Following 20 min of further stirring a white slurry precipitate formed. The solution was evaporated to dryness, and the residue was stored under nitrogen. The pyrrole anion is very sensitive to moisture and air and decomposes after several hours in air to a brown powder. CP/MAS ^{13}C-NMR (50.316 MHz): δ (ppm) = 109.97 (s, C-3,4); 129.71 (s, C-2,5).

Pyridinium Chloride. To 0.5 mL of pyridine-^{15}N (6.25 mmol) was added 2.0 mL of concentrated HCl. The clear solution was then evaporated in high vacuum to yield white, very hygroscopic crystals. The pyridinium chloride was stored under nitrogen. CP/MAS ^{13}C NMR (50.316 MHz): δ (ppm) = 127.53 (s, C-3, 5); 141.08 (s, C-2, 6); 146.29 (s, C-4).

Lithium Imidazolate-^{15}N. To a stirred solution of 0.25 g of imidazole-^{15}N (3.6 mmol) in THF was added 1.6 mL of a 2.5 M butyllithium (4 mmol) solution in hexane at room temperature and under nitrogen. After 5 min the solution turned yellow, and a light yellow precipitate formed. The solution was evaporated, and the residue was stored in vacuum for 30 h at 50 °C to remove THF. CP/MAS ^{13}C-NMR (50.316 MHz): δ(ppm) = 147.8 (s, C-2), 127.9 (s, C-4,5); CP/MAS ^{15}N-NMR (40.55 MHz): δ(ppm) = 158.1 (s, N-1).

Spectroscopy. All chemical shift tensor measurements in the solid samples were made on a Chemagnetics CMX-400 spectrometer using either an APEX 5 mm or a 7.5 mm PENCIL rotor probe operating at a nitrogen frequency of 40.55 MHz. The two liquid samples, pyridine and pyrrole, were transferred to 5 mm glass NMR tubes where they were freeze−pump−thawed and sealed. These liquid samples were then placed in a 5 mm probe and cooled with the variable temperature control system to −100 °C (melting points: pyridine −42 °C; pyrrole −24 °C) to freeze the samples. The synthesized compounds were loaded into a rotor in a nitrogen glove bag to prevent contact with air or moisture. All samples were run with standard CP pulse sequences that include a flip-back pulse and echoes so that the powder patterns could be phased adequately with zero order phasing. The proton decoupling power (γB_2) was 78 kHz in the 5 mm probe and 62 kHz in the 7.5 mm probe. The proton power was reduced during the contact time to obtain an adequate Hartmann−Hahn match with nitrogen. The contact times varied from 0.5 to 100 ms, depending on the compound, with pulse delays of 3 to 60 s. The spectral widths were either 40 or 80 kHz and had a digital resolution of 1.9 ppm. The spinning speed was varied during CP/MAS experiments from 3000 to 5000 Hz to discriminate the peak corresponding to the isotropic shift from the side bands.

The proton T_1 was measured on several of the compounds by saturation recovery. The resulting values are as follows: pyridinium cation, 133 s; pyrrole anion, 13 s; imidazole anion, 7.0 s; imidazole, >180 s. These values have an estimated error in the range of 10%. Variable contact time experiments were also run on several of the compounds with the contact time varied from 5 μs to 50 ms. The cross polarization curves were fit with standard techniques to one or two magnetization transfer components[16] on both the T_{NH} (hydrogen/nitrogen cross polarization time constant) and $^HT_{1\rho}$ (proton rotating frame relaxation time) side of the curve. The pyridinium cation is the only compound studied that exhibits a biexponential component in $^HT_{1\rho}$, e.g., 4.9 (81%) ms and 32 (19%) ms. All of the other compounds have $^HT_{1\rho}$ values greater than 100 ms. The corresponding T_{NH} values (and percent contribution from the various mono- and biexponential components in parentheses) are as follows: pyridinium ion (**6-p**), 41 (33%) μs and 469 (67%) μs; pyrrole anion (**5-n**), 2.3 (100%) ms; imidazole anion (**5-n**), 641 (23%) μs and 4.3 (77%) ms; imidazole **5-p**, 44 (57%) μs and 359 (43%) μs; and imidazole **5-n**, 2.2 (100%) ms. The relative errors in these variable contact time measurements may be as large as 25%.

The principal values of the chemical shift tensors were obtained by fitting the static powder patterns using the POWDER method as described previously.[17] Each powder pattern was fit using two different approaches; the traditional method of locking the isotropic shift to the

(9) Anderson-Altmann, K. L.; Phung, C. G.; Mavromoustakos, S.; Zheng, Z.; Facelli, J. C.; Poulter, C. D.; Grant, D. M. *J. Phys. Chem.* **1995**, *99*, 10454.

(10) Anderson-Altmann, K. L. Ph.D. Dissertation, University of Utah, 1994.

(11) Curtis, R. D; Hilborn, J. W.; Wu, G.; Lumsden, M. D.; Wasylishen, R. E.; Pincock, J. A. *J. Phys. Chem.* **1993**, *97*, 1856.

(12) Lumsden, M. D.; Wu, G.; Wasylishen, R. E.; Curtis, R. D. *J. Am. Chem.* Soc. **1993**, *115*, 2825.

(13) Barrie, P. J.; Groombridge, C. J.; Mason, J.; Moore, E. A. *Chem. Phys. Lett.* **1994**, *219*, 491.

(14) Thunus; L.; Delarge, J. J. *Pharm. Belg.* **1966**, *21*, 485.

(15) Staab, H. A.; Wendel, K.; Datta, S. P. *Liebigs Ann. Chem.* **1966**, *694*, 78.

(16) Orendt, A. M.; Solum, M. S.; Sethi, N. K.; Pugmire, R. J.; Grant, D. M. In *Advances in Coal Spectroscopy*; Meuzelaar, H. L., Ed.; Plenum: New York, 1992.

(17) Alderman, D. W.; Solum, M. S.; Grant, D. G. *J. Chem. Phys.* **1986**, *84*, 3717.

Table 1. Experimental Principal Values of ^{15}N Chemical Shifts in Heterocycles[a]

	δ_{11}	δ_{22}	δ_{33}	δ_{iso}	δ_{MAS}	δ_{liq}
pyridine	200	33	−422	−63		−54 to −96
pyridinium	−30	−97	−381	−169	−169.3	−179 to −187
N-methylpyridinium	−25	−141	−363	−176	−175.5	−178.2
pyridine *N*-oxide	29	−42	−287	−100	−98.3	−76 to −107
pyrrole	−136	−234	−328	−233		−224 to −233
pyrrole anion	−39	−90	−372	−167	−165.5	−156
imidazole (N)	19	−55	−359	−132	−134.7	−168 to −186[b]
imidazole (N−H)	−118	−186	−320	−208	−205.7	
imidazole anion	7	−61	−367	−140	−142.3	−176 to −156
imidazole cation	−131	−153	−337	−207	−203.0	−206 to −207
benzimidazole (N)	12	−92	−353	−144	−143.9	−185[c]
benzimidazole (N−H)	−140	−217	−312	−223	−221.8	−237[c]

[a] All principal values in rank order are referenced to neat nitromethane at room temperature. δ_{iso} is the average of the principal components, δ_{MAS} is the isotropic value from a MAS spectrum, and δ_{liq} is the solution isotropic shift taken from the literature.[3] [b] Average for the N and N−H chemical shifts. [c] 185 ppm is the average for the N and N−H resonances in acetone, −237 ppm in DMSO assigned to the N−H resonance.

value obtained from an MAS experiment and, alternatively, obtaining the best fit to the powder pattern without any constraint on the isotropic shift value. The results from the latter method are reported in Table 1. The two fitting procedures yield variations in δ_{av} of 1−4 ppm and, while variations in individual principal values were in the same range, a 10 ppm variation was noted for δ_{33} in the imidazole cation.

Quantum Mechanical Calculations. Density Functional Theory (DFT) calculations of the chemical shifts were performed with the Gaussian 94 computer program.[18] All calculations employed the GIAO[19] (Gauge Invariant Atomic Orbitals) method with Dunning D95** basis sets,[20] which include polarization functions. The DFT calculations use the BLYP exchange correlation functional[21] and a coupled perturbative scheme without including the magnetic field effects in the exchange correlation functional.[22] Calculations were performed for isolated molecules using optimized structures without taking into account intermolecular interactions. In the case of imidazole, however, calculations were also performed for the isolated molecule and for a pair of imidazole molecules using the molecular structure obtained from neutron diffraction data[23] which includes the positions of the hydrogens. The calculations on the imidazole pair were used to obtain an estimate of the intermolecular effects on the ^{15}N chemical shifts of this compound. The calculated chemical shieldings were converted to the shift scale by subtracting the shielding values from the absolute shielding value of nitromethane, −135.8 ppm, given in the literature.[24]

Results and Discussion

The experimentally determined ^{15}N chemical shift principal values, obtained from the unconstrained fitting method, are given in Table 1 and are presented in rank order since powder pattern data cannot be used to assign spacially the principal values onto the molecular frame. For purposes of comparison, the isotropic chemical shifts from MAS spectra recorded in this work and the liquid values taken from the literature are also given in the table. The isotropic chemical shifts derived from the principal values are within 1−4 ppm of the MAS values. Most of the isotropic values derived from the static spectra and from the MAS spectra of the compounds studied exhibit significant differences from the liquid or solution values reported in the literature. In most cases the solid state values are within the range of values reported in the literature for various solvents. These differences between liquid and isotropic solid state ^{15}N chemical shifts are larger than those observed in ^{13}C chemical shifts. Such differences are not surprising and emphasize the importance of intermolecular effects on the nitrogen chemical shifts. The magnitude of these effects is a matter of present study in this laboratory.[5] The values reported for pyridine differ significantly from those reported in an earlier experiment by Schweitzer and Spiess where proton decoupling was not attempted.[25]

The orientation of the principal values on the molecular frame is critical to the chemical interpretation of the shift tensor values. This information has traditionally been obtained from either single crystal experiments or through dipolar correlation experiments. However, in many cases it is not possible to grow adequate single crystals, or, in the case of the liquid samples that must be frozen, the acquisition of the dipolar information required to determine the orientation is quite difficult. In such cases, the shift tensor orientation can be obtained through theoretical techniques such as those employed in this manuscript, and the results obtained on the compounds of interest are given in Table 2. Figure 2 displays the correlation between the calculated (which are given in Table 2) and the experimental principal values of the chemical shift tensors. The standard deviation of the correlation from the best fit line is 37 ppm (We also carried out similar calculations employing Hartree−Fock and MP2 methods but the scatter in the correlations was greater than those obtained with the DFT method.). This scatter is relatively larger by about 5-fold than those observed for ^{13}C chemical shift tensors[26] (approximately 3 ppm over a span of principal values of 250 ppm) even when the larger span of experimental principal values for nitrogen (over 600 ppm) is taken into consideration. This large rms value is consistent with the results observed in previous studies of uracil[9] and benzamide[5] when intermolecular effects are neglected in the calculations. It has been shown that inclusion of intermolecular interactions significantly improves the correlation between experimental and theoretical results.[5,9]

Utilizing the structural information for imidazole obtained from neutron diffraction data[23] it is possible to improve the chemical shift calculations and to examine the effects of

(18) Gaussian 94 (Revision A.1); Frisch, M. J.; Trucks, G. W.; Schlegel, H. B.; Gill, P. M. W.; Johnson, B. G.; Robb, M. A.; Cheeseman, J. R.; Keith, T. A.; Petersson, G. A.; Montgomery, J. A.; Raghavachari, K.; Al-Laham, M. A.; Zakrzewski, V. G.; Ortiz, J. V.; Foresman, J. B.; Cioslowski, J.; Stefanov, B. B.; Nanayakkara, A.; Challacombe, M.; Peng, C. Y.; Ayala, P. Y.; Chen, W.; Wong, M. W.; Andres, J. L.; Replogle, E. S.; Gomperts, R.; Martin, R. L.; Fox, D. J.; Binkley, J. S.; Defrees, D. J.; Baker, J.; Stewart, J. P.; Head-Gordon, M.; Gonzalez, C.; Pople, J. A. Gaussian, Inc.: Pittsburgh, PA, 1995.

(19) Ditchfield, R. *Mol. Phys.* **1974**, *27*, 789.

(20) Dunning, T. H.; Hay, P. J. In *Modern Theoretical Chemistry*; Schaefer III, H. F., Ed.; Plenum: New York, 1976; p 1.

(21) Lee, C.; Yang, W.; Parr, R. G. *Phys. Rev.* **1988**, *B37*, 785 and Becke, A. D. *Phys. Rev.* **1988**, *A38*, 3098.

(22) Cheeseman, J. R.; Trucks, G. W.; Keith, T. A.; Frisch, M. J. *J. Chem. Phys.* **1996**, *104*, 5497.

(23) Craven, B. M.; Mc Mullan, R. K.; Bell, J. D.; Freeman, H. C. *Acta Crystallogr.* **1977**, *B33*, 2585.

(24) Jameson, J. C.; Mason, J. In *Multinuclear NMR*; Mason, J., Ed.; Plenum: New York, 1987; p 56.

(25) Schweitzer, D; Spiess, H. W. *J. Magn. Reson.* **1974**, *15*, 529.

(26) Grant, D. M.; Liu, F.; Iuliucci, R. J.; Phung, C. G.; Facelli, J. C.; Alderman, D. W. *Acta Crystallogr.* **1995**, *B51*, 540.

Table 2. Comparison between Experimental and Calculated ^{15}N Chemical Shifts Principal Values

	δ_t		δ_r		$\delta_\perp$	
			A. Six-Membered Heterocycles[a]			
pyridine	200	(240)	33	(34)	−422	(−409)
pyridinium	−97	(−182)	−30	(−44)	−381	(−344)
N-methylpyridinium	−141	(−138)	−25	(−26)	−363	(−336)
N-pyridineoxide	−42	(28)	29	(34)	−287	(−258)
			B. Five-Membered Heterocycles[a]			
pyrrole	−234	(−240)	−136	(−138)	−328	(−310)
pyrrole anion	−39	(72)	−90	(−43)	−372	(−364)
imidazole (N)	19	(96)	−55	(−33)	−359	(−374)
imidazole (N−H)	−186	(−242)	−118	(−117)	−320	(−306)
imidazole anion	7	(38)	−61	(−39)	−367	(−354)
imidazole cation	−153	(−202)	−131	(−101)	−337	(−319)
			C. Benzimidazole[a]			
benzimidazole (N)	12	(71)	−92	(−62)	−353	(−366)
benzimidazole (N−H)	−217	(−262)	−140	(−152)	−312	(−291)

[a] All values referenced to nitromethane as explained in the text. Values given between parenthesis correspond to the calculated values using the DFT method. The orientation of the experimental principal components have been assigned following the calculated results (see text and Chart 1).

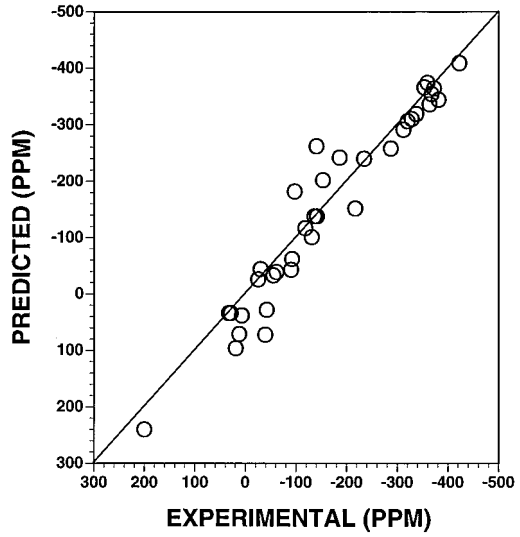

Figure 2. Correlation between the calculated and experimental ^{15}N chemical shift tensor principal values in heterocycles using the Density Functional Theory (DFT) methods. The RMS, slope, and intercept are 37 ppm, 1.05, and 21 ppm, respectively.

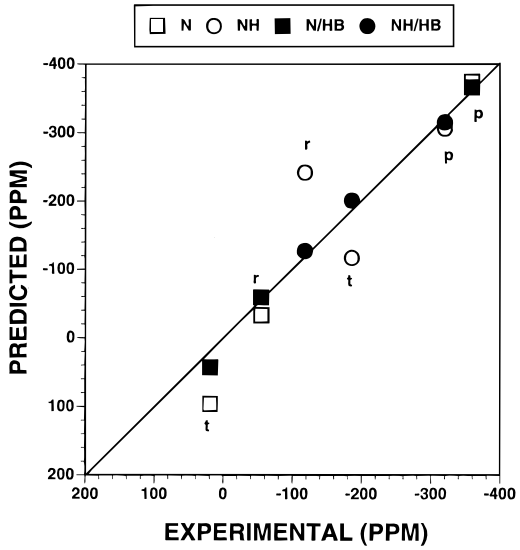

Figure 3. Experimental versus predicted chemical shift values for imidazole. The DFT method was used to calculate the ^{15}N shift tensor values using the neutron diffraction structure and including the effects of intermolecular interactions due to hydrogen bonding. The letters r, t, and p refer to the radial, tangential, and perpendicular components of theshift tensors. The legends N/HB and NH/HB designate predictions based on intermolecular interactions due to hydrogen bonding for the **5-n** and **5-p** nitrogens, respectively, as described in the text.

hydrogen bonding on the ^{15}N shift principal values using the dimeric model described above. The correlation between experimental and calculated shift principal values in imidazole, with and without intermolecular interactions, is displayed in Figure 3. The rms error of the predicted shift principal values is 40.9 ppm using an optimized geometry and is 13.8 ppm when the structural data includes the position of hydrogens in the lattice structure along with the effect of hydrogen bonding. Note, using the experimental structure without including the intermolecular hydrogen bonding effects produces only a modest improvement in the calulated values (rms error is 36.8 ppm) over those obtained with the optimized geometry. The dramatic improvement in the correlation between the experimental and calculated chemical shifts upon including the intermolecular effects suggests that the large rms scatter observed in Figure 2 may be attributed to the isolated molecule approach used in the calculations. The lack of neutron diffraction structural information for the remaining compounds precludes the general approach used in imidazole to improve the calculations. In spite of the relatively large rms, however, the calculations using optimized geometries are adequate to establish the geometrical assignments of the principal shift components onto a molecular frame (see below). Based on previous work on uracil[9] the error

Chart 1. Orientation of the in Plane Principal Components in Heterocycles[a]

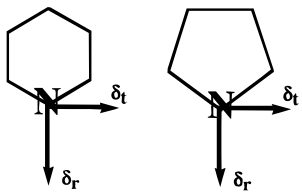

[a] δ_t and δ_r are depicted in the figure and lie in the plane of the ring approximately in the tangential and radial directions of the ring. $\delta_\perp$ is perpendicular to the ring.

in angles between the experimental and predicted components is estimated to be ±10 degrees.

In Table 2 the experimental principal values are compared with the calculated values, and the principal values have been arranged according to their spatial orientation in the molecular frame (see Chart 1). The spacial orientations of the shift tensor on the molecular frame are unavailable from the experimental

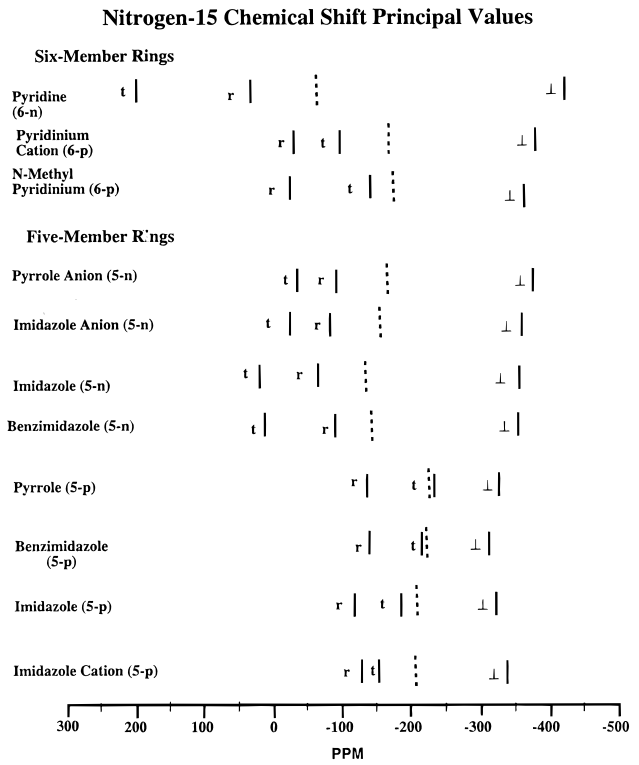

Figure 4. Correlation of the ^{15}N chemical shift tensor principal values in heterocycles. The principal values are marked by solid lines, and the symbols indicate their approximate orientation in the molecular frames as described in the scheme. The isotropic values are given by the dotted lines. The assignment of the principal values in the molecular frame was done according to the quantum mechanical calculations as explained in the text. The designation of **5-n**, **5-p**, **6-n**, and **6-p** nitrogens is described in the text.

data; hence, the calculated orientations were employed to make the assignments. In compounds for which the nitrogen site has less than the required two symmetry planes to specify the orientations, the labeling in the table indicates only the approximate orientations of the principal axes. The calculations predict that the deviations (only a few degrees) from these symmetry orientations are minor, and, therefore, the labeling scheme is assumed to be adequate. Efforts are now underway to obtain single crystal data on some of the compounds studied in order to verify this assumption.

Figure 4 presents a correlation diagram of the principal values of several the ^{15}N chemical shift tensors included in this study. The data have been grouped into the four classes of nitrogen atoms: **6-n**, **6-p**, **5-n**, and **5-p**. Even though only a single example of type **6-n** is shown, additional data obtained in our laboratory indicate that the span of the shift principal values in pyridine (622 ppm) is not unique (e.g., in 4-nitropyridine the principal values of the **6-n** nitrogen are $\delta_{11} = 249$ ppm, $\delta_{22} = 25$ ppm, $\delta_{33} = -425$ ppm, with a span of 674 ppm). A cursory inspection of the figure illustrates the differences in the spans of the principal values in these four nitrogen types. In pyridine one observes that the largest shift component, δ_{11}, is oriented tangential to the ring, a direction that is also perpendicular to the nitrogen lone pair (see Figure 5). When the hybridization of the nitrogen is changed from the **6-n** to the **6-p** type either by protonation, alkylation, or by *N*-oxide formation, not shown, the largest component, δ_{11}, is oriented along the radial direction, and the span of the tensor components is reduced substantially (to a range of 338−351 ppm). The data for the N−CH_3 pyridinium species follow very closely the results of pyridinium hydrochloride. The principal values of pyridine *N*-oxide are

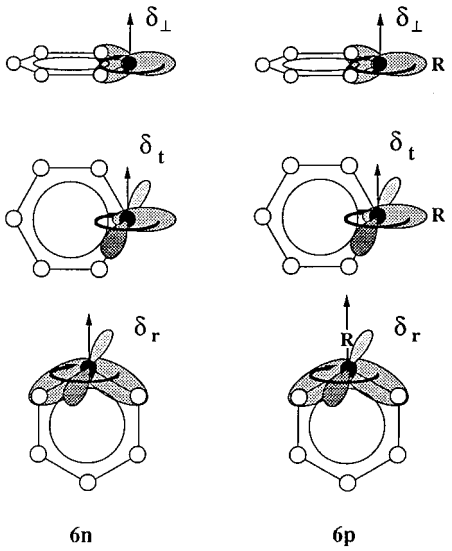

Figure 5. Electron orbitals making the largest contributions to the chemical shift principal components in pyridine. R corresponds to the lone pair in pyridine and R = H, O, or CH_3 in pyridine hydrochloride, *N*-methylpyridine, and *N*-pyridine oxide, respectively.

also similar to the chemical shift components of the pyridinium and *N*-methyl cations but are shifted down field by the replacement of the hydrogen (or methyl) on the lone pair of electrons by an oxygen atom.

The orientation of the shift tensor on the molecular frame of the compounds containing **5-n** type nitrogens corresponds to that found in pyridine (**6-n**). The span of **5-n** tensor components is 336−374 ppm, a range that is nearly identical to that of the **6-p** type nitrogens. In a manner similar to that noted for pyridine, protonation of the **5-n** lone pair inverts the order of the radial and tangential components and also significantly reduces the span of the **5-p** type nitrogens (to a range of 172−206 ppm). This reduction span for the **5-n** and **5-p** species, compared to the respective **6-n** and **6-p** species, may be attributed to the larger degree of localization of the six π-electrons in five-membered heterocycles compared with the corresponding six-membered rings.[27] The increase of the localization of the π-electrons increases the electronic repulsion energy, thereby increasing the energy gaps corresponding to the $\sigma-\pi^*$ and $\pi-\sigma^*$ orbitals which dominate the paramagnetic contribution to the in-plane components. Thus, the paramagnetic contribution to the in-plane components of the shielding term decreases which reduces the shift tensor span.

The isotropic shifts (shown as dashed lines) are also displayed in Figure 4 for each molecule. It is interesting to note that the range of isotropic shift values for all species is 170 ppm but is only 90 ppm if the value of pyridine is not included. Hence, it is clear that even with the large range of isotropic chemical shifts for different nitrogen species, the changes in the chemical shift principal values are much larger than the changes in isotropic shifts and provide much more structurally sensitive information.

The dramatic differences in the nitrogen tensors upon changes of the nitrogen hybridization may be rationalized as follows. It is known that the largest shielding component, δ_{11}, generally orients perpendicular to the plane defined by the bonding−antibonding or HOMO−LUMO pair of orbitals with the smallest energy gap.[28,29] This orientation is a consequence of mixing

(27) Facelli, J. C.; Contreras, R. H. ; Kowalewski, D. G. de ; Kowalewski, V. J.; Piegaia, R. N *J. Mol. Struct. THEOCHEM* **1983**, *94*, 163.
(28) Facelli, J. C; Grant, D. M; Michl, J. *Int. J. Quant. Chem.* **1987**, *31*, 45.

in the occupied and vacant molecular orbitals by the angular momentum operator, specified in the Ramsey expression of the chemical shift.[30,31] Because the paramagnetic term in the Ramsey expression is inversely proportional to the energy gap between the pair of orbitals, the term with the smallest energy gap makes the largest paramagnetic contribution, and the largest chemical shift component is oriented perpendicular to these two orbitals.

A pictorial representation of the orbitals making the largest contributions to the nitrogen shielding principal components in pyridine and its derivatives is given in Figure 5. The tangential component is dominated by the n$-\pi^*$ (lone-pair) transition for the **6-n** nitrogen, while the $\sigma_{N-R}-\pi^*$ transistion dominates this shielding direction for the **6-p** nitrogens. Because the energy gap corresponding to the n$-\pi^*$ transition is quite small, the tangential component becomes the largest chemical shift component (δ_{11}) for the **6-n** nitrogens. In N-substituted compounds the tangential component, δ_t, is dominated by the $\sigma_{N-R}-\pi^*$ transition which has a much larger energy gap, and this shift component becomes $\sim$300 ppm smaller, thereby resulting in a cross component, δ_t, which is designated δ_{22}. Note, δ_r is dominated by the $\sigma_{N-C}-\pi^*$ transitions for both types of nitrogens, **6-n** and **6-p**, because these transitions are not generally affected by protonation. The values of δ_r remain quite similar in both **6-n** and **6-p** nitrogens. The $\delta_\perp$ component, perpendicular to the ring, is dominated by the σ-electronic structure and is not affected by these considerations. This smallest component, δ_{33}, always remains relatively invariant in all the compounds studied. This component, for a given ring size, is also larger (further downfield) for the **p**-type nitrogens than for the corresponding **n**-type nitrogens in the compounds studied. Similar trends are observed in the ^{13}C shift tensors in aromatic compounds, i.e., the perpendicular shift components of protonated and alkyl substituted aromatic carbons are larger than those of aromatic bridgehead carbons.[32]

While the orientation of the ^{15}N chemical shift tensor principal values of pyrrole and pyrrole anion follow the same pattern as that observed in the pyridine compounds, all of the in-plane components are significantly smaller than those of the six-membered ring compounds. The crossover of the tangential and radial components can be explained with the same n$-\pi^*$ and $\sigma_{N-R}-\pi^*$ arguments used for the pyridine compounds.

Imidazole is an interesting case because the neutral species has both **5-n** and **5-p** nitrogens. The tangential component is the largest for **5-n**, while the radial component is the largest for **5-p**. The perpendicular component, $\delta_\perp$, of the **5-p** nitrogen is larger than that of the **5-n** nitrogen but both remain within the narrow range of the δ_{33} components. The orientations and relative magnitudes of the components of the shift tensors of the **5-n** and **5-p** nitrogens in benzimidazole follow the same patterns as those observed in imidazole. For both charged species of imidazole the two nitrogen tensors become equivalent, and their principal values resemble those of the individual **5-p** and **5-n** nitrogens in the parent compound for the cation and anion, respectively. Since the tensor components of benzimidazole follow the same trends exhibited by imidazole, it appears that the benzene ring does not play a major role in determining the overall characteristics of the nitrogen chemical shift tensors.

Conclusions

This paper illustrates the complexity of the chemical shift tensors in nitrogen heterocycles and describes four different types of tensors in five- and six-membered rings. The data show that the ^{15}N chemical shift tensors in heterocyclic compounds are very sensitive to the hybridization of the nitrogen atom and that changes in the tangential component can vary from 200 to as much as 340 ppm in five- and six-membered rings, respectively, when the nitrogen lone-pair hybridization changes. The changes in the magnitude of the in-plane components associated with the protonation state of the nitrogen are so large that these effects may provide a very useful means for probing intermolecular interactions associated with hydrogen bonding in biological systems. It has also been demonstrated that it is possible to measure and spatially assign the principal components of ^{15}N chemical shift tensors obtained from powder samples in heterocyclic compounds. Theoretical predictions of the chemical shift tensors without including intermolecular effects, while of lower quality, are adequate to provide the spatial assignments with confidence. These assignments of the chemical shift principal components are critical for analyzing the relationship between the electronic structure and shift tensors. In all the compounds studied, the largest shift component, δ_{11}, is in the plane of the molecule and approximately perpendicular to the plane containing the bonding$-$antibonding or HOMO$-$LUMO pair of orbitals with the smallest energy gap. The smallest shift component, δ_{33}, is always perpendicular to the plane of the ring, as in the ^{13}C tensors of aromatic compounds, and it is less sensitive to changes in the hybridization of the nitrogen atom than the principal components in the plane of the ring.

Acknowledgment. This work was supported by the U.S. Department of Energy under DOE No. DE-FG02-94ER-1445, the National Institutes of Health, Division of General Medical Sciences, No. GM08521-35, and the NSF through the Advanced Combustion Engineering Research Center. Purchases of ^{15}N enriched compounds were made possible by an educational support grant from the Exxon Corporation. Computer time for this project was provided by an allocation from the University of Utah Center for High Performance Computing.

JA964135+

(29) Solum, M. S.; Facelli, J. C.; Michl, J.; Grant, D. M. *J. Am. Chem Soc.* **1986**, *108*, 6464.

(30) Facelli, J. C. Shielding Calculations: Perturbation Methods. In *Encyclopedia of Nuclear Magnetic Resonance*; Grant, D. M., Harris, R. K., Eds.; John Wiley: London, 1996; p 4299.

(31) Ramsey, N. F. *Phys. Rev.* **1950**, *77*, 567; **1950**, *78*, 699.

(32) Iuliucci, R. J.; Phung, C. G.; Facelli, J. C.; Grant, D. M. *J . Am. Chem. Soc.* **1996**, *118*, 4880.